

Cloning and characterization of a novel Mg^{2+}/H^{+} exchanger

Orit Shaul¹, Donald W. Hilgemann²,
Janice de-Almeida-Engler³,
Marc Van Montagu³, Dirk Inzé^{3,4} and
Gad Galili

Department of Plant Sciences, The Weizmann Institute of Science, Rehovot 76100, Israel, ²Department of Physiology, University of Texas Southwestern Medical Center, TX 75235, USA, ³Laboratorium voor Genetica, Department of Genetics, Flanders Interuniversity Institute for Biotechnology, Universiteit Gent, B-9000 Gent, Belgium and ⁴Laboratoire Associé de l'Institut National de la Recherche Agronomique, France

¹Corresponding author
e-mail: lpshaul@wiccmail.weizmann.ac.il

Cellular functions require adequate homeostasis of several divalent metal cations, including Mg^{2+} and Zn^{2+} . Mg^{2+} , the most abundant free divalent cytoplasmic cation, is essential for many enzymatic reactions, while Zn^{2+} is a structural constituent of various enzymes. Multicellular organisms have to balance not only the intake of Mg^{2+} and Zn^{2+} , but also the distribution of these ions to various organs. To date, genes encoding Mg^{2+} transport proteins have not been cloned from any multicellular organism. We report here the cloning and characterization of an *Arabidopsis thaliana* transporter, designated AtMHX, which is localized in the vacuolar membrane and functions as an electrogenic exchanger of protons with Mg^{2+} and Zn^{2+} ions. Functional homologs of AtMHX have not been cloned from any organism. Ectopic overexpression of AtMHX in transgenic tobacco plants render them sensitive to growth on media containing elevated levels of Mg^{2+} or Zn^{2+} , but does not affect the total amounts of these minerals in shoots of the transgenic plants. AtMHX mRNA is mainly found at the vascular cylinder, and a large proportion of the mRNA is localized in close association with the xylem tracheary elements. This localization suggests that AtMHX may control the partitioning of Mg^{2+} and Zn^{2+} between the various plant organs.

Keywords: *Arabidopsis*/magnesium–proton exchanger/sodium–calcium exchanger/xylem parenchyma/zinc–proton exchanger

Introduction

In all living organisms, cellular functions require a fine homeostasis of various ions and nutrients, including Mg^{2+} and Zn^{2+} . Mg^{2+} is required for the function of many enzymes (e.g. phosphatases, ATPases and RNA polymerases). Zn^{2+} plays both a functional (catalytic) and structural role in several enzyme reactions, and is involved in the regulation of gene expression by zinc-finger proteins.

Both Mg^{2+} and Zn^{2+} are essential for the structural integrity of ribosomes. In plants, Mg^{2+} is also an essential component of chlorophyll, and regulates the activity of key chloroplastic enzymes.

Multicellular organisms have to balance not only their Mg^{2+} and Zn^{2+} intake and intracellular compartmentalization, but also the distribution of these ions to various organs. The movement of ions through membrane barriers is mediated by specialized proteins in the form of channels, transporters or ATPases. So far, genes encoding Mg^{2+} transporters have been cloned only from bacteria and yeast. The bacterial MgtA and MgtB Mg^{2+} transport proteins are P-type ATPases (Hmiel *et al.*, 1989). Mg^{2+} is also transported by the bacterial CorA and mgtE proteins (Smith *et al.*, 1993, 1995), and by the yeast ALR homologs of bacterial CorA (MacDiarmid and Gardner, 1998), but the molecular mechanism of Mg^{2+} mobilization by these proteins is not known. Among the Zn^{2+} transport proteins whose genes have been cloned, the bacterial ZntA (Rensing *et al.*, 1997) is a P-type ATPase. Zn^{2+} is also transported by the yeast ZRT 1,2 (Zhao and Eide, 1996a,b), the *Arabidopsis* ZIP 1–4 (Grotz *et al.*, 1998) and the mammalian ZnT 1–4 (McMahon and Cousins, 1998) transporters, but the molecular mechanism of Zn^{2+} transport by these proteins is also unknown. A mammalian protein designated DCT1 (Gunshin *et al.*, 1997), which belongs to the Nramp family of macrophage proteins, was suggested to be a symporter of protons with various divalent metal cations, including Fe^{2+} and Zn^{2+} , but was not able to symport Mg^{2+} ions.

Little is known about transport proteins that control Mg^{2+} and Zn^{2+} homeostasis in plants. While the proteins mediating Mg^{2+} uptake into roots are unknown, Zn^{2+} transporters, which are induced by Zn^{2+} deficiency and are probably involved in Zn^{2+} uptake, have recently been cloned from *Arabidopsis* (Grotz *et al.*, 1998). Ions absorbed into the cytosol of root cells diffuse towards the vascular cylinder through plasmodesmata and reach the xylem parenchyma cell layer, which borders the xylem vessels. The xylem parenchyma cells were suggested to play a key role in ion secretion into the xylem (xylem loading) and in the release of ions from the xylem (unloading) (Marschner, 1995). These processes require transport through the plasma membrane of the xylem parenchyma cells, but the proteins mediating xylem loading and unloading of Mg^{2+} and Zn^{2+} are not known. Unloaded Mg^{2+} and Zn^{2+} subsequently enter the surrounding cells through unknown transport proteins. The molecular mechanisms of phloem loading and unloading with Mg^{2+} and Zn^{2+} have also not been elucidated. Intracellularly, the vacuole is considered the main organelle mediating Mg^{2+} homeostasis in the cytosol and the chloroplast. Vacuolar Mg^{2+} is also important for the cation–anion balance and turgor regulation of cells (Marschner,

1995). The activity of a Mg^{2+}/H^{+} antiporter was identified in luteoid (vacuolar) vesicles of *Hevea brasiliensis* (Amalou *et al.*, 1992, 1994) and in vacuolar membranes from roots of *Zea mays* L. (Pfeiffer and Hager, 1993), but cloning of the corresponding genes has not been reported. The *H. brasiliensis* transporter was indicated to be electro-neutral and to be capable of transporting also Zn^{2+} cations. In Zn^{2+} -tolerant species, tolerance is achieved mainly by sequestering Zn^{2+} in the vacuoles (Brookes *et al.*, 1981), but the transport mechanism is not known.

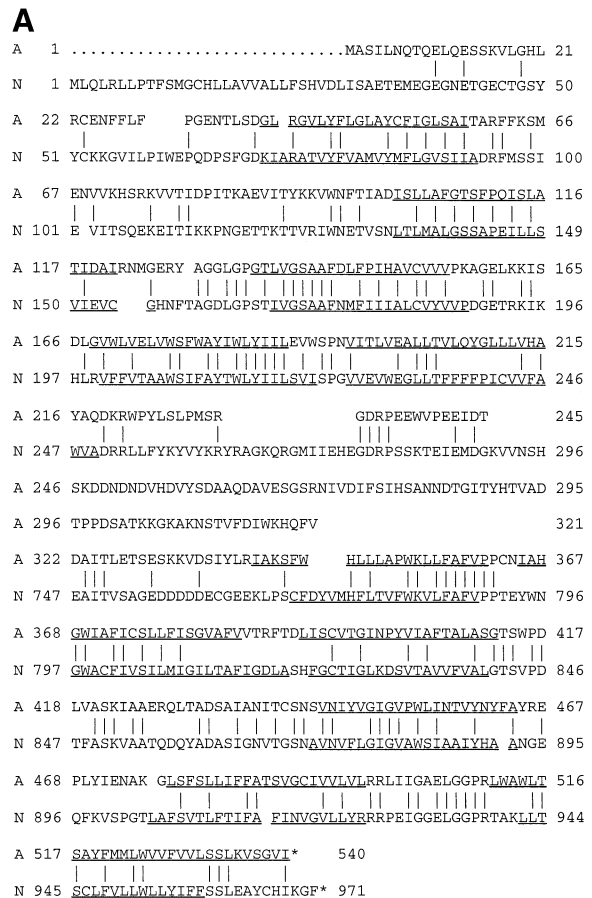
We describe here the cloning and characterization of an *Arabidopsis* transporter, designated AtMHX, that is localized in the vacuolar membrane and functions as an electrogenic exchanger of protons with Mg^{2+} and Zn^{2+} ions. To our knowledge, genes encoding Mg^{2+}/H^{+} or Zn^{2+}/H^{+} exchangers have not yet been cloned from any organism. The main site of AtMHX transcription is the vascular cylinder, suggesting that it plays a role in Mg^{2+} and Zn^{2+} partitioning between the various plant organs.

Results

Cloning of AtMHX

Using a PCR approach, we isolated an *Arabidopsis* cDNA fragment whose deduced amino acid sequence showed homology to NCX1, a mammalian Na^{+}/Ca^{2+} exchanger (Nicoll *et al.*, 1990). In animal cells, NCX1 plays a major role in extrusion of Ca^{2+} ions to the extracellular space following excitation. Considering that homologs of animal Na^{+}/Ca^{2+} exchangers have not been characterized from any plant species, we aimed to determine the role of the plant protein, and cloned its entire cDNA and genomic DNA (these sequences have been submitted to the DDBJ/EMBL/GenBank database under accession Nos AF109178 and AF109182, respectively). The deduced protein encoded by this gene, later designated AtMHX, showed 36% identity to NCX1 (Figure 1A). Hydrophobicity plots indicate that the two proteins share structural similarity (Figure 1B). Both AtMHX and NCX1 contain 11 putative transmembrane spans, which parallel each other throughout the whole sequence (Figure 1A). In addition, both proteins have a long non-membranal loop between transmembrane spans 5 and 6. In NCX1, this loop is 500 amino acids (aa) long and is not essential for the transport function, but has a regulatory role; in AtMHX this loop is much shorter, being only 100 aa in length.

We used the coding-sequence of AtMHX as a probe for low-stringency Southern blot hybridization of genomic *Arabidopsis* DNA, which has been digested with restriction enzymes whose recognition sequences appear only at the 5' or 3' non-coding regions (Figure 2). The appearance of a single hybridization band suggested that AtMHX is encoded by a single gene in *Arabidopsis*. Comparison between the cDNA and genomic clones showed that the *AtMHX* gene includes eight introns (data not shown). The first intron is 414 bp long and resides within the 5' untranslated region (5' UTR), while the other introns range between 70 and 148 bp. We have used the inverse PCR technique (Triglia *et al.*, 1988) to obtain part of the 5' upstream region of the *AtMHX* gene. To identify the site of transcription initiation within this sequence, we used the 5' RACE system (Clontech) as described previously (Liu and Gorovsky, 1993), with slight modifications. In



B

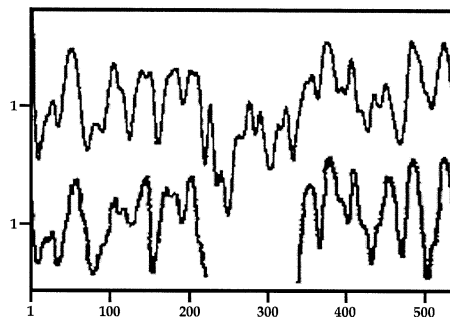


Fig. 1. (A) Comparison between the deduced amino acid sequences of AtMHX (A, upper rows) and NCX1 (N, lower rows). Most of the non-membranal loop of NCX1 (between amino acids 297–746) is not shown. The transmembrane spans, as predicted by the Eisenberg, Schwarz, Komarony and Wall method (Eisenberg *et al.*, 1984), are underlined. (B) Hydrophobicity plot of AtMHX (upper line) and NCX1 (lower line). The non-membranal loop of NCX1 is not shown. The numbers on the x-axis correspond to the amino-acid sequence of AtMHX. The numbers on the y-axis correspond to the hydrophobicity of each protein separately.

short, a synthetic single-stranded anchor primer was ligated at the 3' position of an *Arabidopsis* first-strand cDNA pool. PCR fragments were amplified using a 5' gene-specific primer, and at least 20 of the resulting clones were sequenced. The longest clones included an additional G residue at the 5' terminus of the anchor primer, which did not reside from the sequences of either the anchor primer or the upstream region of the *AtMHX* gene. This G residue reflected the position of the 5'-CAP of the cDNA, and indicated that the transcription initiation site

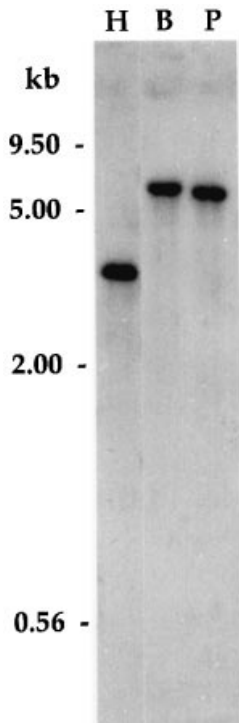


Fig. 2. Low-stringency Southern blot hybridization of genomic *Arabidopsis* DNA with the AtMHX coding region. The genomic DNA was cut with *HincII* (H), *BamHI* (B), or *PvuI* (P), whose recognition sequence appear only in the 3' or 5' non-coding regions of the genomic DNA clone.

```

                -74
1  ACGCTTGAAT CCTCGTTTCG ATACAATAAT TGAAGTGTGT CATGCAGAGA
                -34                +1
51  TTAGAGAGAT GTGTATAAAT GGCTCCCAAG TCTCCACCGC AATATCCAAC
101  GCTTGACCGA TTCCAATCAG CTCCTCTCGA TTTCCGTTTG TCGGAAAATC
151  TCTCCCGTGA TCGGGGTATT GTGAATGCCG CTCACCGAGA TATTCTCCGG
201  TACGTCGCGA TTGATCAATT TCGTCGCGTG GCTCACTCTG TTTCATCTGT
251  TCTTTTCTTA TTTTTTAGCT ATTTTGTGTTG AGATTGTGTC GTTGAAAATT
301  ATGTTTTTGT GAAAAGAACC CAACTTGTGT TACTGAACCC ATGATGAAAG
351  TTATAATCTT TTGATCTGGT TACCTCTGGA TTTTGATTAC GCATACAGTG
401  GAACATGCAA TTGTATTATAG CATTGGTTAT AGATTGGATT TCGGTTACAT
451  GCCATTGGAT CCGTGCAAT GTTTAGTTTG TGTACAGAT TCTCTGAAAA
501  GAAATCTTTT TGCATGTTC GTTTGTTCG CATCCTCTTG ATACTGTTTG
551  ATCGATCAGG CTACAGGTTT CATCAGTTTC TTCTAAAAGT TGTAAGCTTC
601  TTTTTGGTGT GCCAGATTCT TTTCCCAGT GAGGACAAGT GTTCAATTGA
                MET
651  CTTATTAGGA GGTGGGTTT GAATAAGTTA CAATGGCCTC AATCTTAAAT
    
```

Fig. 3. The 5' upstream region of the *AtMHX* gene. The 414 bp intron in the non-coding region is underlined. Double-underlined are the transcription initiation site at position +1, the putative CAAT and TATA boxes at positions -74 and -34, respectively, and the initiating ATG codon (MET).

is located at 575 bp upstream to the initiating ATG codon (Figure 3). Typical CAAT and TATA boxes are located at positions -74 and -34, respectively, relative to the transcription initiation site (Figure 3). After *AtMHX* was cloned in our laboratory, its genomic DNA sequence was also found on chromosome II in the frame of the *Arabidopsis* genome project (DDBJ/EMBL/GenBank accession No. AC002535), and its partial deduced amino

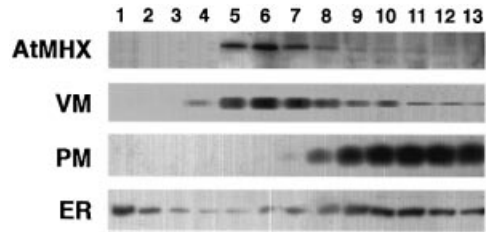


Fig. 4. Intracellular localization of AtMHX in wild-type *Arabidopsis* plants. *Arabidopsis* root membranes were extracted and fractionated in sucrose gradient as previously described (Schaller and DeWitt, 1995). The fractions (fraction 1 = 20% sucrose; fraction 13 = 45% sucrose) were subjected to Western blot analyses with the following antibodies: AtMHX, affinity-purified antibodies against a peptide from AtMHX deduced amino-acid sequence; VM, antibodies against a vacuolar membrane marker [VM23, a homolog of γ -TIP from radish (*Raphanus sativus*), which is a species closely related to *Arabidopsis* (Maeshima, 1992)]; PM, antibodies against the *Arabidopsis* plasma membrane marker protein RD-28 (Yamaguchi-Shinozaki *et al.*, 1992); ER, antibodies against the endoplasmic reticulum yeast BiP protein, that specifically recognize plant ER BiP (Shimoni *et al.*, 1995).

acid sequence, translated from an internal methionine, has also been annotated to have similarity to the $\text{Na}^+/\text{Ca}^{2+}$ exchanger.

AtMHX is localized in the vacuolar membrane

AtMHX contains 11 putative transmembrane spans (Figure 1), but lacks any special sequences that could suggest in which cellular membrane it is localized. *NCX1* is localized in the plasma membrane and includes a cleaved signal peptide, which is, however, not essential for its localization (Sahin-Toth *et al.*, 1995). Alignment of the deduced amino-acid sequences of *AtMHX* and *NCX1* (Figure 1A) shows that *AtMHX* initiates around the cleavage point of the *NCX1* signal peptide, located 32 residues downstream from the *NCX1* initiating methionine. To identify the cellular localization of *AtMHX*, we produced polyclonal antibodies against a peptide from the deduced amino acid sequence of its central non-membranal loop. These antibodies were purified further against the same peptide. Fractionation of *Arabidopsis* membranes on sucrose gradient, followed by Western blot analysis, showed that *AtMHX* co-fractionates with the vacuolar membrane marker γ -TIP, and not with plasma membrane or ER markers (Figure 4). Similarly, it did not co-fractionate with mitochondria, plastids or nuclei, as indicated by differential centrifugation (data not shown). *AtMHX* is thus localized in the vacuolar membrane. This localization was supported by our electrophysiological analyses in membranes of tobacco cells transformed with the *AtMHX* gene (see below).

AtMHX exchanges protons with Mg^{2+} , Zn^{2+} and Fe^{2+} ions

To identify the function of *AtMHX*, we overexpressed it under control of the strong constitutive 35S promoter (Guilley, 1982) and the Ω enhancer of translation (Gallie *et al.*, 1987) in two independently transformed tobacco BY-2 cell lines, each composed of a heterogeneous mixture of transformed cells (Nagata *et al.*, 1992; Shaul *et al.*, 1996). The two transgenic cell lines produced a protein with the expected mol. wt of 54 kDa, which did not appear in control, non-transformed cells (data not shown). Similar to wild-type *Arabidopsis* plants, *AtMHX* co-migrated in

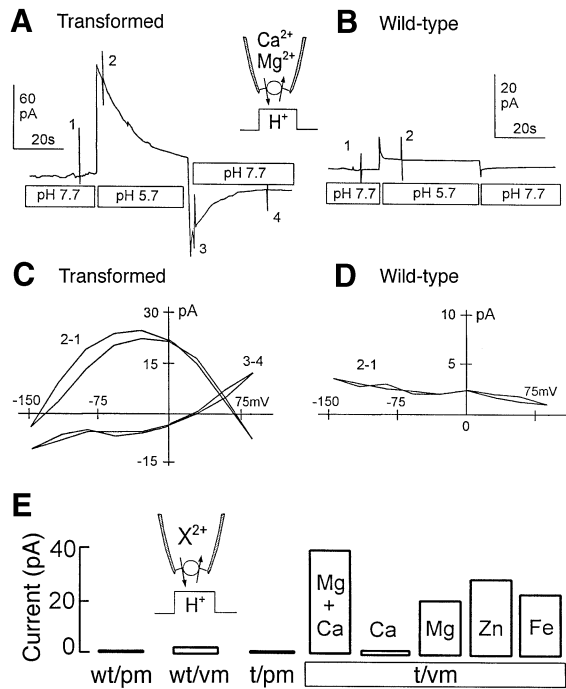


Fig. 5. Proton-activated currents associated with AtMHX expression in vacuolar giant patches. (A) Patch from a vacuole of a transformed cell. Currents are activated by switching from a pH 7.7 solution to a pH 5.7 solution and back to pH 7.7. *N*-methyl-glucamine (NMG) is the only monovalent cation in solution. The pipette solution (pH 7.0; cytoplasmic membrane side) contains 2 mM Mg^{2+} and 2 mM Ca^{2+} ; the bath solution contains 0.5 mM Mg^{2+} . (B) Typical current records for the same protocol in a vacuolar patch from a non-transformed cell. (C) Current–voltage relations for the proton-activated current in Figure 5A ('2-1'), whereby records were subtracted just before (1) and after (2) application of the pH 5.7 solution. In addition, the current–voltage relation is given for the reverse current observed on removing protons, whereby the subtracted records were obtained just after returning to pH 7.7 (3) and 30 s later when the current had decayed (4). (D) Current–voltage relation of the 10 times smaller current activated by the same protocol in a giant patch from a non-transformed cell. (E) Average magnitudes of 2–4 proton activated currents in giant patches from vacuolar membrane (vm) and plasma membranes (pm) from wild-type (wt) and transformed (t) cells. In vacuolar patches from transformed cells (t/vm) currents are largest with 2 mM Mg^{2+} and 2 mM Ca^{2+} in the pipette ('Mg+Ca'); 2 mM Ca^{2+} alone did not support a current; currents activated with 2 mM Mg^{2+} , 0.2 mM Zn^{2+} and 0.2 mM Fe^{2+} in the pipette are similar in magnitude. No significant currents were obtained in plasma membrane patches of transformed cells (t/pm) or in membrane patches of wild-type cells (wt/pm, wt/vm) with either of these solutions in the pipette (the currents shown for wt/pm, wt/vm and t/pm were measures with 2 mM Mg^{2+} and 2 mM Ca^{2+} in the pipette).

sucrose density gradients with the vacuolar membrane marker of the transformed BY-2 cells (data not shown), indicating that it was transported to the vacuole also in the transformed tobacco cells.

To determine whether AtMHX carries out electrogenic ion transport, we studied ionic currents in giant patches (8–12 μm) (Hilgemann, 1995; Hilgemann and Lu, 1998) from both the plasma membrane and from vacuoles of transformed and non-transformed cells. Similar results were obtained in the two independently transformed cultures. Tests for $\text{Na}^+/\text{Ca}^{2+}$ exchange currents and Na^+ - or Ca^{2+} -activated conductances were entirely negative. As shown in Figure 5, large currents were activated by applying acidic solutions (pH 5.7) to the exposed (intravacuolar) membrane surface of vacuolar patches from

transformed cells (Figure 5A). Solutions on both membrane sides contained only *N*-methyl-glucamine (NMG) as monovalent cation. Current activation required the presence of Mg^{2+} , but not Ca^{2+} in the pipette (Figure 5E), which strongly suggests an electrogenic $\text{Mg}^{2+}/\text{H}^+$ exchange process. Vacuolar patches from non-transformed cells (Figure 5B and E) or patches from the plasma membrane of either transformed or non-transformed cells (Figure 5E) gave almost no current response, supporting the localization of AtMHX in the vacuolar membrane. The current activated by low pH decayed substantially over 30 s (Figure 5A), a kinetic property reminiscent of bovine cardiac $\text{Na}^+/\text{Ca}^{2+}$ exchange inactivation (Hilgemann, 1990). A current of opposite sign was activated transiently when the control solution (pH 7.7) was applied. This might reflect reverse $\text{Mg}^{2+}/\text{H}^+$ exchange because there is a 6-fold proton gradient opposing a 4-fold Mg^{2+} gradient (pipette solution, 2 mM Mg^{2+} at pH 7.0; bath solution, 0.5 mM Mg^{2+} at pH 7.7). The current–voltage relation of the proton-activated current (subtraction of records 1 and 2 in Figure 5A) showed a 'U' shape (Figure 5C), and the reverse current also shows a complex voltage dependence. These wave forms may reflect the presence of two electrogenic ion translocation steps with opposite voltage-dependence. Current–voltage relations in vacuolar patches from non-transformed cells were very shallow in comparison and were monotonic (Figure 5D). The outward current activated by protons was larger when 2 mM Ca^{2+} was also included in the pipette ($n = 3$), although 2 mM Ca^{2+} alone supported no current ($n = 4$; Figure 5E). Activation was also seen with 50 μM Ca^{2+} in the pipette (data not shown), but no activation was observed when Ca^{2+} was applied to the exposed (intravacuolar) membrane surface of vacuolar patches. Activation by cytoplasmic Ca^{2+} is another property reminiscent of the bovine cardiac $\text{Na}^+/\text{Ca}^{2+}$ exchanger (Hilgemann, 1990). Both Zn^{2+} (0.2 mM) and Fe^{2+} (0.2 mM) supported proton-activated current when they were included in the pipette instead of Mg^{2+} (Figure 5E), whilst Co^{2+} , Ni^{2+} and Cu^{2+} did not support current (data not shown). From these results we conclude that AtMHX is an electrogenic $\text{Mg}^{2+}/\text{H}^+$ exchanger in the vacuolar membrane, but it may also transport other divalent metals. Those that support current, Zn^{2+} and Fe^{2+} , are of similar ionic radius to Mg^{2+} . Since under physiological conditions iron is almost exclusively found in complexes in plant cells (Marschner, 1995), Fe^{2+} ions are unlikely to be transported in significant amounts by AtMHX *in vivo*.

AtMHX apparently functions in Mg^{2+} and Zn^{2+} transport in planta

Following the electrophysiological analyses, we wished to ascertain whether AtMHX can also function as a Mg^{2+} and Zn^{2+} transporter *in planta*. To address this, we overexpressed AtMHX in transgenic tobacco plants under control of the 35S promoter and the Ω enhancer of translation. Three independently transformed lines which overexpressed a protein with the expected mol. wt (Figure 6) were selected for further study. The overexpressed protein co-migrated in sucrose density gradients with the vacuolar membrane marker of tobacco plants (data not shown). When grown in tissue culture plates in medium supplemented with excess Mg^{2+} or Zn^{2+} ions,

C 9 2 1

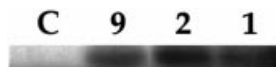


Fig. 6. Western blot of transformed tobacco plants with anti-AtMHX antibodies. Twenty micrograms of protein were loaded on each lane. C, a non-transformed tobacco plant; 1, 2 and 9, three independently transformed tobacco lines.

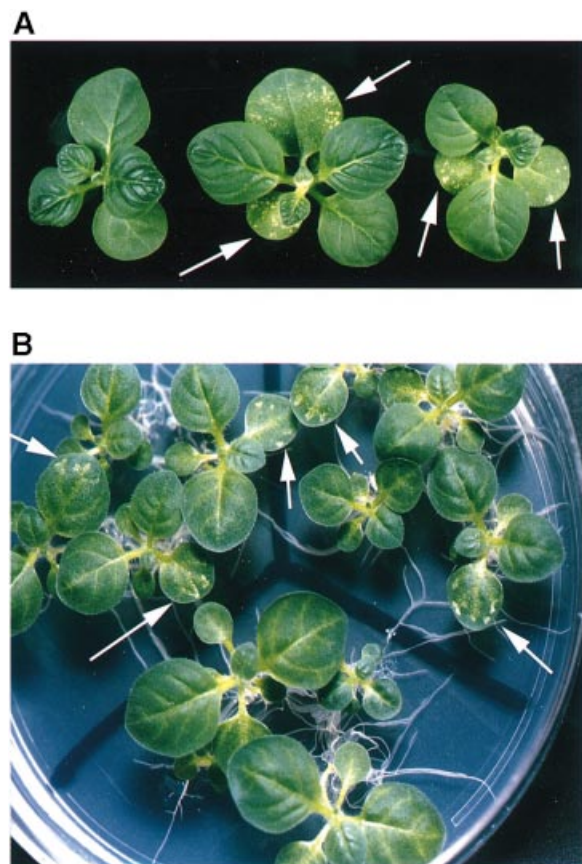


Fig. 7. The phenotype of transgenic tobacco plants grown on medium containing elevated levels of Mg^{2+} or Zn^{2+} . (A) Shoots of tobacco plants that were grown in tissue culture in Nitsch medium (Nitsch, 1969) containing 60 mM Mg_2SO_4 (compared with 0.75 mM in a standard Nitsch medium). Arrows indicate the necrotic lesions in the two independent transgenic tobacco lines 2 (right) and 9 (middle), which do not appear in the non-transformed plant (left). (B) Tobacco plants grown in a tissue culture plate in Nitsch medium containing 0.175 mM Zn_2SO_4 (compared with 0.035 mM in a standard Nitsch medium). The plate was divided to three zones: bottom, non-transformed plants; upper, the two transgenic lines 2 (right) and 9 (left). Arrows indicate the necrotic lesions in leaves of the transgenic plants.

the three transgenic tobacco lines exhibited necrotic lesions in their leaves, which were not observed in wild-type plants grown under the same conditions (an example is shown in Figure 7). Similar lesions did not appear in transgenic tobacco plants grown in the presence of high concentrations of other cations, or equal concentrations of the accompanying anions with different cations (data not shown). These findings suggest that AtMHX is also capable of transporting Mg^{2+} and Zn^{2+} in planta.

Next, we wished to study whether AtMHX overexpression affects the accumulation of magnesium or zinc in the plants. Interestingly, no difference was observed in the total content of these minerals between shoots of trans-

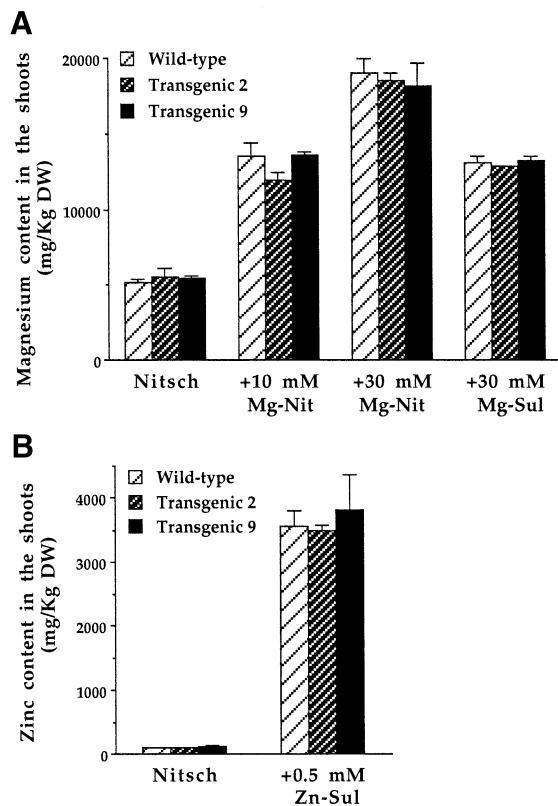


Fig. 8. Magnesium and zinc content in shoots of plants grown in plates including high levels of these minerals. Each plate included 12 seedlings, whose aerial parts were pooled before analysis. Each column represents the average \pm SD of four plates for the wild-type plants, or two plates for each of the two independently transformed lines 2 and 9. (A) Magnesium content in shoots of plants grown in Nitsch medium (Nitsch, 1969) containing standard Mg^{2+} levels (0.75 mM Mg_2SO_4), or with the indicated levels of $Mg(NO_3)_2$ (Mg-Nit) or Mg_2SO_4 (Mg-Sul). (B) Zinc content in shoots of plants grown in Nitsch medium containing standard Zn^{2+} levels (0.035 mM Zn_2SO_4), or with 0.5 mM Zn_2SO_4 (Zn-Sul).

formed and non-transformed plants (Figure 8). The amounts of magnesium or zinc increased to similar levels in shoots of transformed and non-transformed plants upon growth in media containing elevated levels of these minerals (Figure 8).

AtMHX mRNA is mainly associated with the xylem tracheary elements of all plant organs

Northern blots showed that AtMHX mRNA is more abundant in *Arabidopsis* roots, stems and inflorescence than in leaves (Figure 9). *In situ* hybridization analysis was carried out to delineate the sites of expression (Figure 10). In cross sections of roots and stems, expression was seen in the vascular cylinder (Figure 10A and B). Expression could also be seen in the root epidermis. In longitudinal sections of all plant organs (roots, stems, leaves, inflorescence and siliques), intense staining was observed in close proximity to the xylem tracheary elements (e.g. Figure 10C–H). No signal was observed in this region upon hybridization with sense probes (data not shown). In addition, expression could be observed in meristematic regions and in very young leaves (data not shown). Altogether, we observed that in all mature plant organs, AtMHX mRNA is found mainly at the vascular cylinder, and a large proportion of the mRNA is localized

in close association with the xylem tracheary elements. As differentiated tracheary elements are dead cells, the expression should reside at the living cell layers that border the xylem tracheary elements, such as the xylem parenchyma. However, expression of AtMHX in other cell layers of the vascular cylinder cannot be excluded.

Discussion

We report here the characterization of an *Arabidopsis* transporter, AtMHX, which is the first Mg^{2+} transporter to be cloned from a multicellular organism, and the first cloned exchanger of protons with Mg^{2+} and Zn^{2+} ions. Although AtMHX shows limited sequence homology with animal Na^+/Ca^{2+} exchangers, the two transporter species are functionally distinct. In animals, Na^+/K^+ -ATPases

generate Na^+ gradients that provide the driving force for most transport processes, including Ca^{2+} extrusion from the cytosol to the extracellular space by Na^+/Ca^{2+} exchangers localized in the plasma membrane. In plants, the driving force for most transport processes is the electrochemical H^+ gradient, which is generated by H^+ -ATPases localized in both the plasma membrane and the vacuolar membrane (Maathuis and Sanders, 1992). Notably, in contrast to animal Na^+/Ca^{2+} exchangers, AtMHX is incapable of transporting Ca^{2+} ions, but can serve as an electrogenic exchanger of protons with Mg^{2+} , Zn^{2+} and Fe^{2+} ions. The transport of Mg^{2+} and Zn^{2+} *in vitro* by AtMHX occurs at concentration ranges found in the plant cytosol (i.e. the millimolar range for Mg^{2+} and the micromolar range for Zn^{2+}) (Marschner, 1995). In contrast to Mg^{2+} and Zn^{2+} , iron is almost exclusively found in complexes in plant cells, mostly in the chloroplast (Marschner, 1995), and therefore Fe^{2+} ions are unlikely to be transported in significant amounts by AtMHX *in vivo*. AtMHX is localized in the vacuolar membrane, and as vacuolar pH is lower compared with the cytosol, we expect that under physiological conditions AtMHX transports divalent cations into the vacuole. Our observations that transgenic tobacco plants ectopically overexpressing AtMHX are specifically sensitive to high Mg^{2+} or Zn^{2+} levels support the *in vitro* transport studies, and indicate that this protein is apparently also capable of transporting Mg^{2+} and Zn^{2+} ions *in planta*. Still, overexpression of the transporter did not alter the total content of magnesium or zinc in shoots of the transgenic plants. Upon growth in media containing elevated Mg^{2+} or Zn^{2+} levels, these minerals increased to similar levels in shoots of transformed and non-transformed plants. Thus, further study is necessary to determine the direct cause of necrotic

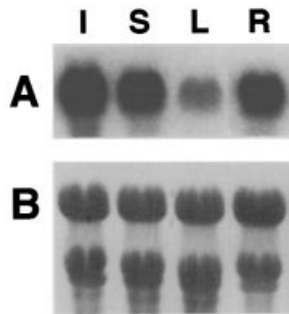


Fig. 9. Northern blot analysis of AtMHX mRNA. RNA was extracted from various *Arabidopsis* tissues and subjected to Northern blot analysis as previously described (Shaul *et al.*, 1996). Twenty micrograms of total RNA were loaded on each lane. (A) Hybridization with the AtMHX coding sequence. (B) Methylene blue staining, showing the levels of RNA loaded. I, inflorescence; S, stems; L, leaves; R, roots.

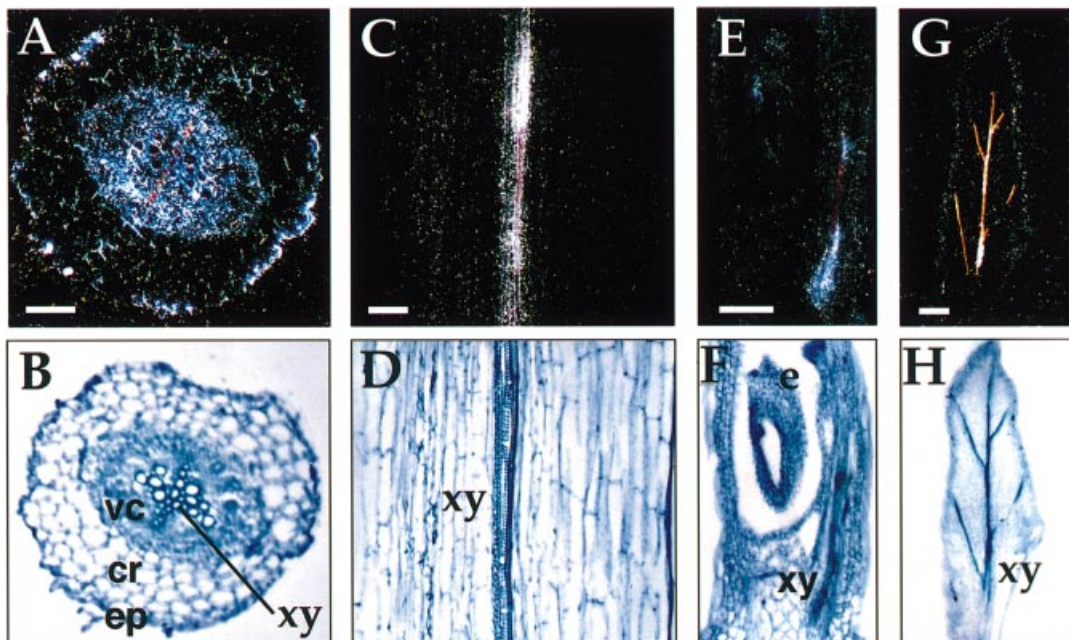


Fig. 10. *In situ* hybridization of AtMHX mRNA. The analyses were performed in both *Arabidopsis* and radish, a closely related species, yielding similar results. (A, C, E, G) Pictures taken in a dark field. The light-colored dots represent the hybridization signal. (B, D, F and H) The same pictures as (A), (C), (E) and (G), respectively, taken in a bright field, showing the toluidine blue staining; the silver-grain hybridization signal may appear as dark dots in bright field. (A, B) Cross section of a radish root. (C, D) Longitudinal section of a radish stem. (E, F) Longitudinal section of an *Arabidopsis* leaf. (G, H) Longitudinal section of an *Arabidopsis* silique. (cr, cortex; e, embryo; ep, epidermis; vc, vascular cylinder; xy, xylem tracheary elements). Bar = 100 μ M.

lesions in leaves of transformed plants grown under such conditions. One possible explanation could be a localized change in the content of Mg^{2+} or Zn^{2+} in the necrotic lesions, which occupy a small part of the total shoot area. An alternative assumption is that, being localized in the internal vacuolar membrane, AtMHX does not change the total amounts of Mg^{2+} or Zn^{2+} in the cells, but can affect their intracellular distribution. Accordingly, under conditions of high cellular Mg^{2+} or Zn^{2+} levels, extensive exchange of these cations with vacuolar protons may impair the cellular pH or ATP balance (the ATP being needed for re-building the pH balance by H^+ -ATPases).

Little is known about the mechanisms regulating Mg^{2+} and Zn^{2+} homeostasis in plants. Imbalance in these ions has severe consequences: Mg^{2+} deficiency impairs the export of carbohydrates from source to sink sites, increases the photosensitivity of leaves and impairs root growth; at the same time, high cytosolic levels of Mg^{2+} inhibit photosynthesis (Marschner, 1995). Zn^{2+} deficiency increases RNA degradation and leads to a drastic reduction in the rate of protein synthesis, while Zn^{2+} toxicity is characterized by chlorosis, and by inhibition in the rate of photosynthesis and root growth (Marschner, 1995). The significant enrichment of AtMHX mRNA at the vascular cylinder of all *Arabidopsis* organs suggests that this transporter plays an important role in controlling Mg^{2+} and Zn^{2+} distribution between the various plant organs. A large proportion of the mRNA is localized in close association with the xylem tracheary elements. As differentiated tracheary elements are dead cells, the expression should reside at the living cell layers that border the xylem tracheary elements, such as the xylem parenchyma. Our working hypothesis for the potential role of AtMHX in the xylem parenchyma cells is related to the function of these cells in loading and unloading of the xylem vessels with minerals and nutrients, and also in reabsorption of certain ions from the xylem sap along the pathway to the shoot (Marschner, 1995). It was shown that the xylem parenchyma (and stem tissue in general) of certain species can reabsorb some minerals (potassium, sodium and nitrate) from the xylem sap in periods of ample root supply, and release these minerals into the xylem sap in periods of insufficient supply (Marschner, 1995). AtMHX may determine the proportion of Mg^{2+} and Zn^{2+} ions to be stored in the vacuoles of the xylem parenchyma cells, and, consequently, their amount available in the cytosol during xylem loading and unloading. According to this hypothesis, AtMHX could function in a buffering capacity, sequestering excess amounts, or creating a vacuolar pool that could be used in periods of deficiency.

Materials and methods

Cloning of AtMHX

A first-strand cDNA prepared from poly(A)⁺ mRNA purified from *A.thaliana* cv. C-24 was employed in a PCR with the following degenerate primers, originally selected for cloning another gene: 5'-CA(C/T)GA(G/A)AA(G/A)GTICA(G/A)GGIGG-3', and 5'-GCC-CA(G/A)TGIA(G/A)IGCIGT(G/A)TG-3'. The resulting cDNA clone, 735 bp in length, included an open reading frame that showed homology to animal Na^+/Ca^{2+} exchangers. To clone the 5' and 3' regions, the 5' and 3' RACE systems of Clontech were employed according to the manufacturer's instructions. To obtain the full-length cDNA, the first-strand cDNA described above was used as a template for a PCR with the following primers: 5'-GGGGGAACGCTTGACCGATTC-3' and

5'-CCGGCCTCCAAAATCATAGT-3'. One microliter of the product of this reaction was used as template for a second PCR with the following nested primers: 5'-CCCGTGATCGGCGTATTGTGA-3' and 5'-GCC-AACTGCCTTTGAACCTTTG-3'. The PCR product including the full length cDNA was ligated into the pGEM-5Zf(+) vector (Promega) that was linearized with *EcoRV* to obtain plasmid p218.

To obtain the genomic clone, total genomic DNA (prepared from *A.thaliana* cv. C-24) was used as a template for two successive PCRs using the same primer-sets used for obtaining the cDNA clone. One microliter of the second PCR was used as template for a third PCR with the following nested primers: 5'-ATGCCGCTACCGAGATATT-3' and 5'-TCTTCTACTCATGGGGTTTTTC-3'.

Preparation of antibodies

Polyclonal antibodies were raised against a synthetic peptide that was derived from AtMHX sequence: Cys Met Ser Arg Gly Asp Arg Pro Glu Glu Trp Val Pro Glu Glu Ile. The peptide was linked through its initial Cys residue to the high-molecular-weight KLH carrier (Calbiochem) as previously described (Harlow and Lane, 1988) and injected to rabbits. The antibodies were affinity purified against this peptide using the SulfoLink Coupling Gel (Pierce) according to manufacturer's instructions.

Expression of AtMHX in tobacco BY-2 cells and tobacco plants

For construction of a chimeric gene for AtMHX expression, plasmid p218 was used as a template for a PCR using an upper primer introducing a *NcoI* site at the initiating ATG codon, 5'-GGGGTTTGAATAA-GTTACCATGGCCTCAATTCTTA-3', and the lower primer 5'-TCT-TCTATATGACGCCTGAAACT-3'. The PCR product was cloned into plasmid pJD330, 3' to the 35S promoter (Guilley, 1982) and to the Ω 5'UTR sequence, previously shown to enhance translation of eukaryotic mRNAs (Gallie *et al.*, 1987), and 5' to the nopaline synthase transcription termination and polyadenylation signals (Holsters *et al.*, 1980). This chimeric gene was cloned into an *Agrobacterium* binary vector, immobilized into *Agrobacterium tumefaciens* C58C1(pMP90), and stably transformed into the tobacco BY-2 cell line (Nagata *et al.*, 1992) as described previously (Shaul *et al.*, 1996). Tobacco Samsun NN plants were transformed with the same *Agrobacterium* strain as described previously (Horsch *et al.*, 1985).

Growth of transformed tobacco plants in medium supplemented with high levels of various ions and mineral content analysis

F₁ seeds of transformed and non-transformed tobacco plants were surface-sterilized and germinated in tissue-culture plates on Nitsch medium (Nitsch, 1969), including kanamycin as a selective agent. Ten-day-old seedlings were transferred with their intact roots to 15-cm diameter plates containing Nitsch medium supplemented with various minerals, as indicated in the text and the legends to Figures 7 and 8. The plants were grown further for 1 month. For mineral content analyses, all the aerial parts were excised from each plant, washed twice in double-distilled water, dried for 48 h in a 70°C oven, and crushed into a fine powder. For each sample, 120–250 mg dry powder was weighed into 50 ml polypropylene disposable test tubes, 5 ml of concentrated nitric acid were added, and after 10 min at room temperature the samples were digested in the microwave. Analyses were conducted on portions of these solutions. Magnesium and zinc content were determined by inductively coupled plasma atomic emission spectrometry. An ICP-AES model 'Spectroflame' from Spectro (Kleve, Germany) was used.

Electrophysiology

Seven-day-old BY-2 cells were treated with 1% cellulase YC and 0.1% pectolyase Y-23 (both from Seishin Pharmaceutical Co., Japan) in 0.4 M mannitol, 10 mM MES, pH 5.5, for ~1 h at room temperature, and then washed twice with the same solution excluding the enzymes. Cells were then incubated for 2 h in a medium containing 0.12 M mannitol, 20 mM KCl, 2 mM $MgCl_2$ and 10 mM HEPES pH 6.8. Vacuoles, which appear as large clear membrane bubbles, were extruded spontaneously by the cells upon placing them in hypotonic medium of the same composition without mannitol. Giant membrane patches were formed by the methods described previously (Hilgemann, 1995; Hilgemann and Lu, 1998). Both the pipette and the bath solutions contained 100 mM *N*-methyl-D-glucamine (NMG), 100 mM MES, 10 mM HEPES, 15 mM Tris, and HCl or NMG to adjust pH. The pipette solution (pH 7.0) contained in addition divalent cations, as indicated in the text and Figure 5, and the bath solution contained in addition 0.5 mM Mg^{2+} . The holding potential

was 0 mV; membrane potential indicates the bath (intravacuolar) membrane side with respect to the pipette (cytoplasmic) membrane side. Current–voltage relations were determined by applying 10 ms cumulative voltage steps in the hyperpolarizing direction, then in the depolarizing direction, and finally back to 0 mV. Records presented are subtractions of the indicated raw current records.

In situ hybridization

In situ hybridization was performed as described previously (Van der Eycken *et al.*, 1996). The radioactive anti-sense probes included the whole AtMHX cDNA and 3' non-coding sequence. Sense probes of the same sequence were used as a control. Photographs were taken with a Diaplan microscope equipped with bright- and dark-field optics (Leitz, Wetzlar, Germany).

Acknowledgements

We thank R. De Groot and S. Feng for expert technical assistance, K. D. Philipson and D. A. Nicoll for testing AtMHX mRNA in *Xenopus* oocytes, Y. Kapulnik, S. Lev-Yadun, D. Aviv, H. Rahamimoff and S. Schuldiner for helpful discussions, Y. Avivi for critical reading of the manuscript, M. Maeshima for the kind gift of anti-radish-VM23 antibodies, M. J. Chrispeels for a kind gift of anti-RD28 antibodies, D. R. Gallie for a kind gift of plasmid pJD330, and the Tobacco Science Research Laboratory, Japan Tobacco, Inc., for permitting us to use the tobacco BY-2 cell-line. D. I. is a Research Director of the Institut National de la Recherche Agronomique (France). G. G. is an incumbent of the Bronfman Chair of Plant Sciences.

References

Amalou, Z., Gibrat, R., Brugidou, C., Trouslot, P. and d'Auzac, J. (1992) Evidence for an amiloride-inhibited $Mg^{2+}/2H^{+}$ antiporter in luteoid (vacuolar) vesicles from latex of *Hevea brasiliensis*. *Plant Physiol.*, **100**, 255–260.

Amalou, Z., Gibrat, R., Trouslot, P. and d'Auzac, J. (1994) Solubilization and reconstitution of the $Mg^{2+}/2H^{+}$ antiporter of the luteoid tonoplast from *Hevea brasiliensis* latex. *Plant Physiol.*, **106**, 79–85.

Brookes, R. R., Collins, J. C. and Thurman, D. A. (1981) The mechanism of zinc tolerance in grasses. *J. Plant Nutr.*, **3**, 695–705.

Eisenberg, D., Schwarz, E., Komaromy, M. and Wall, R. (1984) Analysis of membrane and surface protein sequences with the hydrophobic moment plot. *J. Mol. Biol.*, **179**, 125–142.

Gallie, D. R., Sleat, D. E., Watts, J. W., Turner, P. C. and Wilson, T. M. (1987) The 5'-leader sequence of tobacco mosaic virus RNA enhances the expression of foreign gene transcripts *in vitro* and *in vivo*. *Nucleic Acids Res.*, **15**, 3257–3273.

Grotz, N., Fox, T., Connolly, E., Park, W., Gueriot, M. L. and Eide, D. (1998) Identification of a family of zinc transporter genes from *Arabidopsis* that respond to zinc deficiency. *Proc. Natl Acad. Sci. USA*, **95**, 7220–7224.

Guilley, H. (1982) Transcription of Cauliflower mosaic virus DNA: detection of promoter sequences and characterization of transcripts. *Cell*, **30**, 763–773.

Gunshin, H., Mackenzie, B., Berger, U. V., Gunshin, Y., Romero, M. F., Boron, W. F., Nussberger, S., Gollan, J. L. and Hediger, M. A. (1997) Cloning and characterization of a mammalian proton-coupled metal-ion transporter. *Nature*, **388**, 482–488.

Harlow, E. D. and Lane, D. (1988) *Antibodies: A Laboratory Manual*. Cold Spring Harbor Laboratory Press, Cold Spring Harbor, NY.

Hilgemann, D. W. (1990) Regulation and deregulation of cardiac sodium-calcium exchange in giant excised sarcolemmal patches. *Nature*, **344**, 242–245.

Hilgemann, D. W. (1995) The giant membrane patch. In Sakmann, B. and Neher, E. (eds), *Single Channel Recording*. Plenum Press, New York, NY, pp. 307–327.

Hilgemann, D. W. and Lu, C.-C. (1998) Giant membrane patches: improvements and applications. *Methods Enzymol.*, **293**, 267–280.

Hmiel, S. P., Snavely, M. D., Florer, J. B., Maguire, M. E. and Miller, C. G. (1989) Magnesium transport in *Salmonella typhimurium*: genetic characterization and cloning of three magnesium transport loci. *J. Bacteriol.*, **171**, 4742–4751.

Holsters, M. *et al.* (1980) The functional organization of the nopaline A. *tumefaciens* plasmid pTiC58. *Plasmid*, **3**, 212–230.

Horsch, R. B., Fry, J. E., Hoffmann, N. L., Eichholtz, D., Rogers, S. G. and Fraley, R. T. (1985) A simple and general method for transferring genes into plants. *Science*, **227**, 1229–1231.

Liu, X. and Gorovsky, M. A. (1993) Mapping the 5' and 3' ends of *Tetrahymena thermophila* mRNAs using RNA ligase mediated amplification of cDNA ends (RLM-RACE). *Nucleic Acids Res.*, **21**, 4954–4960.

Maathuis, F. J. M. and Sanders, D. (1992) Plant membrane transport. *Curr. Opin. Cell Biol.*, **4**, 661–669.

MacDiarmid, C. W. and Gardner, R. C. (1998) Overexpression of the *Saccharomyces cerevisiae* magnesium transport system confers resistance to aluminum ion. *J. Biol. Chem.*, **273**, 1727–1732.

Maeshima, M. (1992) Characterization of the major integral protein of vacuolar membrane. *Plant Physiol.*, **98**, 1248–1254.

Marschner, H. (1995) *Mineral Nutrition of Higher Plants*. Academic Press, London, UK.

McMahon, R. J. and Cousins, R. J. (1998) Mammalian zinc transporters. *J. Nutr.*, **128**, 667–670.

Nagata, T., Nemoto, Y. and Hasezawa, S. (1992) Tobacco BY-2 cell line as the 'HeLa' cell in the cell biology of higher plants. *Int. Rev. Cytol.*, **132**, 1–30.

Nicoll, D. A., Longoni, S. and Philipson, K. D. (1990) Molecular cloning and functional expression of the cardiac sarcolemmal Na^{+}/Ca^{2+} exchanger. *Science*, **250**, 562–565.

Nitsch, J. P. (1969) Experimental androgenesis in *Nicotiana*. *Phytomorphology*, **19**, 389–404.

Pfeiffer, W. and Hager, A. (1993) A Ca^{2+} -ATPase and a Mg^{2+}/H^{+} antiporter are present on tonoplast membranes from roots of *Zea mays* L. *Planta*, **191**, 377–385.

Rensing, C., Mitra, B. and Rosen, B. P. (1997) The zntA gene of *Escherichia coli* encodes a Zn (II)-translocating P-type ATPase. *Proc. Natl Acad. Sci. USA*, **94**, 14326–14331.

Sahin-Toth, M., Nicoll, D. A., Frank, J. S., Philipson, K. D. and Friedlander, M. (1995) The cleaved N-terminal signal sequence of the cardiac Na^{+}/Ca^{2+} exchanger is not required for functional membrane integration. *Biochem. Biophys. Res. Commun.*, **212**, 968–974.

Schaller, G. E. and DeWitt, N. D. (1995) Analysis of the H^{+} -ATPase and other proteins of the *Arabidopsis* plasma membrane. *Methods Cell Biol.*, **50**, 129–148.

Shaul, O., Mironov, V., Burssens, S., Van Montagu, M. and Inzé, D. (1996) Two *Arabidopsis* cyclin promoters mediate distinctive transcriptional oscillation in synchronized tobacco BY-2 cells. *Proc. Natl Acad. Sci. USA*, **93**, 4868–4872.

Shimoni, Y., Zhu, X., Levanony, H., Segal, G. and Galili, G. (1995) Purification, characterization and intracellular localization of glycosylated protein disulfide isomerase from wheat grains. *Plant Physiol.*, **108**, 327–335.

Smith, R. L., Banks, J. L., Marshall, D. S. and Maguire, M. E. (1993) Sequence and topology of the CorA magnesium transport systems of *Salmonella typhimurium* and *Escherichia coli*. Identification of a new class of transport proteins. *J. Biol. Chem.*, **268**, 14071–14080.

Smith, R. L., Thompson, L. J. and Maguire, M. E. (1995) Cloning and characterization of *mgtE*, a putative new class of Mg^{2+} transporter from *Bacillus firmus* OF4. *J. Bacteriol.*, **177**, 1233–1238.

Triglia, T., Peterson, M. G. and Kemp, D. J. (1988) A procedure of *in vitro* amplification of DNA segments that lie outside the boundaries of known sequences. *Nucleic Acids Res.*, **16**, 8186.

Van der Eycken, W., de Almeida Engler, J., Inzé, D., Van Montagu, M. and Gheysen, G. (1996) A molecular study of root-knot nematode-induced feeding sites. *Plant J.*, **9**, 45–54.

Yamaguchi-Shinozaki, K., Masahiro, K., Satomi, U. and Kazuo, S. (1992) Molecular cloning and characterization of 9 cDNAs for genes that are responsive for desiccation in *Arabidopsis thaliana*: sequence analysis of one cDNA clone that encodes a putative transmembrane channel protein. *Plant Cell Physiol.*, **33**, 217–224.

Zhao, H. and Eide, D. (1996a) The yeast ZRT1 gene encodes the zinc transporter protein of a high-affinity uptake system induced by zinc limitation. *Proc. Natl Acad. Sci. USA*, **93**, 2454–2458.

Zhao, H. and Eide, D. (1996b) The ZRT2 gene encodes the low affinity zinc transporter in *Saccharomyces cerevisiae*. *J. Biol. Chem.*, **271**, 23203–23210.

Received January 20, 1999; revised May 24, 1999;
accepted June 3, 1999